

Computational Evaluation of Spray Characteristics in Pressure Swirl Atomizers

Arun S, Rakesh P

Department of Mechanical Engineering
College of Engineering Trivandrum (CET) Thiruvananthapuram
aruntvm100@gmail.com
rakp73@gmail.com

Abstract— Pressure swirl atomizers are used to obtain improved atomization and mixing efficiency due to their wider spray cone angles. In these atomizers, the liquid to be atomized enters through tangential inlets producing a swirling motion inside a swirl chamber and creates a central air core surrounded by a liquid sheet that spreads radially outward to form a hollow cone spray. In this work, a computational study of the spray emanating from a pressure swirl atomizer is done using Ansys Fluent by 3-D modelling of the atomizer nozzle along with the external spray domain and the spray characteristics like Sauter Mean Diameter (SMD), spray cone angle, droplet diameter distribution, particle tracking, etc. for various injection conditions are measured and analysed numerically, and validated with the theoretical estimates. The variation of the spray characteristics at various injection conditions is analysed numerically, to find the optimum operating conditions of the injector and its effect on the overall atomizer performance. Particle trajectories of the spray particles is determined using the Discrete Phase Model (DPM) in a Lagrangian reference frame.

Keywords— swirl number; sheet break-up; droplet diameter; Sauter Mean Diameter; Discrete Phase Model; particle tracks

NOMENCLATURE

m_L	- mass flow rate of the liquid (kg/s)
ρ_L	- Density of the liquid (kg/m ³)
ΔP_L	- Injector pressure differential (bar)
D_s	- Diameter of the swirl chamber (mm)
D_0	- Nozzle exit orifice diameter (mm)
L_s	- Length of the swirl Chamber (mm)
D_P	- Diameter of the tangential entry port (mm)
L_s	- Length of the tangential entry port (mm)
h_0	- Liquid sheet thickness at the nozzle tip (mm)
U_0	- Velocity of the liquid at the atomizer tip (m/s)
D_L	- Ligament diameter (mm)
C_d	- Discharge coefficient (Dimensionless constant)
K_A	- Atomizer Constant (Dimensionless constant)
K_V	- Velocity Coefficient (Dimensionless constant)
θ	- Spray semi angle

I. INTRODUCTION

The process of breaking or atomization of the liquid fuel into tiny droplets in the form of a fine spray plays a vital role in various industrial and propulsion applications. During the combustion process of liquid propellants in an engine, the increase in surface area of liquid volume encountered during the atomization process alters several parameters: increasing volumetric heat release rate, easier light up of the mixture of fuel and oxidizer, reducing the exhaust concentrations of pollutant emissions, etc. In this context the study of sprays and the design of injection systems assume great importance.

To produce a good atomization, a high relative velocity between the liquid to be atomized and the surrounding air or gas is required. In pressure swirl atomizers, a separate swirl chamber with tangential slots or swirl piece (with helical or tangential passages) is provided upstream of the circular exit orifice. Due to swirling motion provided to the liquid, an air core is formed, which is surrounded by the liquid sheet that emerges from the orifice as a thinning sheet, which is unstable, breaking up into ligaments and droplets. Swirl number is used to characterize such atomizers, which is the ratio of circumferential velocity of liquid to its axial velocity. As swirl number increases spray cone angle also increases. Atomization quality goes up with the increasing injection pressure and spray cone angle. The pressure swirl atomizer, also known as 'simplex atomizer' with its dimensions are shown in figure 1.

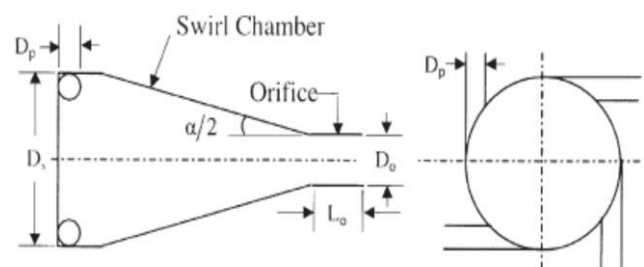


Fig. 1. Schematics of Pressure Swirl Atomizer [1]

For some applications a spray in the form of a solid cone is preferred. This can be achieved by using an axial jet or with the

use of other mechanical devices to inject droplets into the center of the hollow conical spray pattern produced by the swirl chamber. These two methods of injection create a bimodal distribution of drop sizes, with the droplets concentrated at the center of the spray generally larger than those near the edge.

Two main approaches are used in the numerical analysis of multiphase flow in swirl atomizers, Euler-Euler and Euler-Lagrange, of which the latter is used in the present work. In the Euler-Lagrange formulation, the Navier-Stokes equations are solved for the fluid phase, while the dispersed phase is solved by tracking a large number of particles, bubbles, or droplets through the calculated flow field. The dispersed phase can exchange momentum, mass, and energy with the fluid phase. In the computational domain there are two separate phases present, namely the continuous and the discrete phase (particles). The transport equations are solved for the continuous phase only and the motion of particles is dealt with particle trajectory calculations. Through an iterative solution procedure the mass, momentum and energy interaction between both phases can be realized. In order to simulate spray formation, (discrete) liquid particles have to be introduced to interact with the present (continuous) gas phase.

Current design methods and available correlations for prediction of spray characteristics from a simplex nozzle are outlined by Lefebvre [2]. It provides a detailed review of the experimental and theoretical studies on the flow phenomena in atomizers and spray formation. It is also specified that a change in the geometry can significantly alter the performance. There are many semi empirical correlations which are used to provide guidance in designing simplex nozzles.

The Linear Instability Sheet Atomization (LISA) was applied to model the formation of spray droplets of a continuous spray from a pressure swirl atomizer. The secondary breakup of spray droplets was simulated by the Taylor Analogy Breakup (TAB) model. Two way momentum coupling was applied to handle the interaction between the gas and liquid phases. The droplet size distribution from numerical solution agreed with experimental result in literature.

The principle of operation of a pressure swirl (simplex) atomizer and formation of air core is depicted in the figure 2 below.

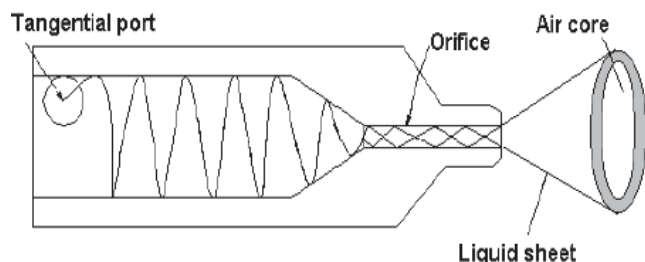


Fig.2. Principle of operation of a simplex atomizer

Swirl motion is imparted to the flowing liquid in the upstream region of fuel orifice. It is done by passing the liquid through tangential orifices. The swirling motion makes the liquid to confine with the walls of the swirl chamber and creates an air-core in the spray axis region. Filmy liquid flow with air-core is seen inside the fuel orifice. At the orifice exit, the

swirling liquid diverges (due to centrifugal force) out in the form of a thin liquid film. The liquid film disintegrates via hydrodynamic instability mechanisms and produces fine droplets.

II. DETERMINATION OF SPRAY CHARACTERISTICS

A. Computation Details

The numerical solution of the model equations and computational simulations have been performed by utilizing a 3D pressure-based solver incorporated in CFD package ANSYS FLUENT 14. The solver is based on the finite volumes technique and enables two-way coupled DPM method for treatment of the continuous and discrete phases. The nozzle geometry and the external domain has been meshed by 169,748 unstructured and structured grid cells of tetrahedral and polyhedral shape with the various mesh sizes. Particularly smaller mesh volumes are located in the regions of high concentration of the discrete phase in the downstream direction of the spray injection, where large gradients of momentum, heat and mass transfer are expected to occur. Correspondingly, grid cells of the larger sizes are located near the top and side walls of the external domain.

The most important dimensions of the pressure swirl atomizer used for the present study are the diameter of the nozzle exit orifice, $D_O = 2$ mm, the swirl chamber diameter, $D_S = 6$ mm, diameter of the tangential entry port, $D_P = 2.472$ mm, length of the nozzle orifice, $L_O = 2$ mm, the tangential entry port length, $L_P = 3.955$ mm, length of the swirl chamber, $L_S = 6$ mm. These dimensions are obtained from the theoretical relations developed and proved experimentally for pressure swirl atomizers.

A mixture containing species including liquid water, air, and water vapor are defined at the external domain, where only air, which is the continuous phase is there initially before solving for the discrete phase trajectories. The fluid which is flowing through the tangential inlets and producing a swirl motion in the swirl chamber and creating a central air core is injected at the nozzle exit orifice into the external domain where atmospheric conditions exist. The fluids used for modelling are liquid water which is the fluid flowing through the tangential inlets and injecting at the nozzle exit orifice, and air is used as the continuous phase, which is filled in the external domain initially before the injection occurs. For all cases, the fluids air and water are taken at room temperature and atmospheric pressure.

The computations are performed on a 3-D full geometry mesh created using ANSYS workbench and the initial and boundary conditions are set. The nozzle and the spray regions are represented within a single calculation domain. The spray domain is rectangular in shape and has dimensions of 35 mm and 70 mm. The mass flow rate through the inlets is selected based on the application and the atomizer dimensions are calculated by using theoretical correlations for pressure swirl atomizers. The computational domain (top half) used in the present study is shown in figure-3 with all regions of flow clearly specified.



Fig. 3. Computational Domain

Inlet boundary condition is selected as mass flow inlet. The nozzle walls has been given the wall boundary condition with specified shear and default values of roughness constant and other constants. The outlet is defined as pressure outlet, as the flow is exiting into the domain where air at atmospheric conditions is filled initially.

The turbulence model used for modeling is realizable k-ε model. This model is used as it gives a more accurate prediction of the spreading rate of both planar and round jets than standard k-ε model. The species transport is enabled and a mixture containing species liquid water, air and water vapor is selected. The initial solution is calculated without the spray droplets. This solution is the solution of the continuous phase, which is the air. The next step is to define the discrete phase modeling (DPM) parameters for creating the spray injection from the atomizer. Taylor Analogy Breakup (TAB) model is selected as the break up model for accounting for the breakup of spray particles in the external domain. The dynamic drag model is applicable in almost any circumstance. It is compatible with both the TAB and wave models for spray breakup.

After setting the discrete phase modelling (DPM) parameters, the properties and type of injections have to be defined. Pressure swirl atomizer model is used to predict the droplet size and velocity distributions. This atomization model uses numerous attributes of the nozzle and spray fluid, such as orifice diameter and mass flow rate etc., to calculate initial droplet size, velocity, and position. For atomizer simulations, the droplets must be randomly distributed, both spatially through a dispersion angle and in their time of release. The atomizer models use stochastic trajectory selection to achieve random distribution.

All the numerical simulations of spray modelling have been performed in steady state two way coupling mode. For continuous phase, the spatial discretization was performed by upwind scheme of second order for all conservation equations and SIMPLE scheme was used for coupling between the pressure and velocity. For the dispersed phase, the tracking scheme is automatically selected between low order implicit and high order trapezoidal schemes based on the solution stability. DPM sources were updated every iteration of the continuous phase. The overall steady-state numerical formulation was of the second order of accuracy.

B. Governing Equations

The continuous phase is always modeled in the Eulerian framework, where the local instantaneous balance equation of

the conserved property being transported is written on an Eulerian control volume which is fixed in the space and allows for flow through its faces. The continuity, momentum (Navier Stokes equations) and energy equations together with the transport equations for species concentrations respectively is given below.

$$\frac{\partial \rho}{\partial t} + \frac{\partial(\rho U_i)}{\partial x_j} = S_m \quad (1)$$

$$\frac{\partial(U_i)}{\partial t} + \sum_j U_j \frac{\partial(U_i)}{\partial x_j} = -\frac{1}{\rho} \frac{\partial P}{\partial x_i} + \sum_j \frac{1}{\rho} \frac{\partial(\tau_{ji})}{\partial x_j} + g_i + S_p \quad (2)$$

$$\begin{aligned} \frac{\partial(\rho C_p T)}{\partial t} + U_j \frac{\partial(\rho C_p T)}{\partial x_j} \\ = k \frac{\partial^2 T}{\partial x_j \partial x_j} - P \frac{\partial U_i}{\partial x_j} + \tau_{kj} \frac{\partial U_k}{\partial x_j} + S_T \end{aligned} \quad (3)$$

$$\frac{\partial(C_n)}{\partial t} + U_j \frac{\partial(C_n)}{\partial x_j} = \frac{\partial}{\partial x_j} \left(D_n \frac{\partial \tau_n}{\partial x_j} \right) + S_n \quad (4)$$

The first and second terms in the above equations are accumulation and advection of the conserved property respectively. S_m , S_p , S_T and S_n are source terms, due to the presence of particles, for mass, momentum, energy and concentration respectively. In the momentum equation, the first and second terms on the right hand side are the gradients of normal and shear stresses of the fluid and the third one represents the effect of body forces. The first term on the right hand side of energy equation represents conductive heat transfer with 'k' being thermal conductivity, neglecting the effect of turbulence. The second and third terms represent the effect of expansion and viscous dissipation respectively. The first term on the right hand side of species transport equation represents species transport due to molecular diffusion.

In addition to solving transport equations for the continuous phase, DPM allows to simulate a discrete second phase in a Lagrangian frame of reference. This second phase consists of spherical particles (which may be taken to represent droplets or bubbles) dispersed in the continuous phase. It also computes the trajectories of the discrete phase entities, as well as heat and mass transfer to/from them. The coupling between the phases and its impact on both the discrete phase trajectories and the continuous phase flow is also included. The dispersion of particles due to turbulence in the fluid phase is predicted using the stochastic tracking model. The stochastic tracking (random walk) model includes the effect of instantaneous turbulent velocity fluctuations on the particle trajectories through the use of stochastic methods.

The discrete phase is modelled by defining the initial position, velocity, size, orifice diameter and temperature of individual particles. These initial conditions, along with inputs defining the physical properties of the discrete phase, are used to initiate trajectory and heat/mass transfer calculations.

The trajectory of a discrete phase particle (or droplet or bubble) is obtained by integrating the force balance on the particle, which is written in a Lagrangian reference frame. This force balance equates the particle inertia with the forces acting

on the particle, and can be written (for the x direction in Cartesian coordinates) as

$$\frac{du_p}{dt} = F_{D_{u-u_p}} + \frac{g_x(\rho-\rho_p)}{\rho_p} + F_x \quad (5)$$

Where $F_{D_{u-u_p}}$ is the drag force per unit particle mass and $F_x = F_{pressure} + F_{virtual\ mass} + F_{gravity} + F_{other}$ is the additional force.

$$\text{Drag Force, } F_D = \frac{18\mu}{\rho_p d_p^2} \frac{C_D Re}{24} \quad (6)$$

Here, u is the fluid phase velocity, u_p is the particle velocity, μ is the molecular viscosity of the fluid, ρ is the fluid density, ρ_p is the density of the particle, and d_p is the particle diameter. Re is the relative Reynolds number, which is defined as

$$Re = \frac{\rho d_p |u_p - u|}{\mu} \quad (7)$$

The drag coefficient C_D is defined by

$$C_D = a_1 + \frac{a_2}{Re} + \frac{a_3}{Re^2} \quad (8)$$

Where a_1 , a_2 , and a_3 are constants that apply for smooth spherical particles over several ranges of Reynolds number, Re .

As the trajectory of a particle is computed, a track of the heat, mass, and momentum gained or lost by the particle stream that follows that trajectory and these quantities are incorporated in the subsequent continuous phase calculations. Thus, while the continuous phase always impacts the discrete phase, we can also incorporate the effect of the discrete phase trajectories on the continuum. This two-way coupling is accomplished by alternately solving the discrete and continuous phase equations until the solutions in both phases have stopped changing.

C. Theoretical Estimation and Validation

There are several empirical and semi-empirical correlations for designing pressure swirl atomizers and to find the spray characteristics. These correlations, which are modified for pressure swirl atomizers are validated with the experimental observations and found to be in excellent agreement by Pedro Teixeira Lacava et al. [3].

Flow number (FN) is calculated by the equation

$$FN = \frac{\dot{m}_L}{\sqrt{(\rho_L \Delta P_L)}} \quad (9)$$

Where \dot{m}_L is the liquid mass flow rate, ρ_L is the liquid density, and ΔP_L is the injector pressure differential.

The nozzle discharge diameter (D_0) is chosen and the remaining atomizer geometrical parameters are obtained considering the following dimensionless groups: $\left(\frac{A_p}{D_s D_0}\right)$, $\left(\frac{D_s}{D_0}\right)$, $\left(\frac{L_s}{D_s}\right)$, $\left(\frac{L_0}{D_0}\right)$, and $\left(\frac{L_p}{D_p}\right)$; where A_p is the tangential entry passage cross section area.

Discharge coefficient is calculated by the equation

$$C_d = \frac{\dot{m}_L}{A_0 \sqrt{(2\rho_L \Delta P_L)}} \quad (10)$$

The ratios $\left(\frac{A_p}{D_s D_0}\right)$, and $\left(\frac{D_s}{D_0}\right)$, can be obtained from empirical relation

$$C_d = 0.35 \left(\frac{D_s}{D_0}\right)^{0.5} \left(\frac{A_p}{D_s D_0}\right)^{0.25} \quad (11)$$

The spray semi angle (θ) can be estimated by the relation

$$\sin \theta = \frac{\frac{\pi}{2} C_D}{K(1+\sqrt{X})} \quad (12)$$

Where $K = \left(\frac{A_p}{D_s D_0}\right)$ and 'X' is the ratio between the air core area (A_a) and the nozzle orifice exit area (A_0), estimated by equation below

$$D_0 = 2 \sqrt{\frac{FN}{\pi(1-X)\sqrt{2}}} \quad (13)$$

With the flow number (FN) and the spray semiangle (θ), obtained earlier, it is possible to estimate the liquid sheet thickness at the nozzle tip, h_0

The liquid sheet thickness at the nozzle tip is given by the expression

$$h_0 = \frac{0.00805 FN \sqrt{\rho_L}}{D_0 \cos \theta} \quad (14)$$

Nozzle exit diameter (D_0) and area (A_0) can be found out by the relation.

$$D_0 = 2 \sqrt{\frac{FN}{\pi(1-X)\sqrt{2}}} \quad (15)$$

Ligament diameter (D_L) is given by

$$D_L = 0.9615 \cos \theta \left(\frac{h_0^4 \sigma^2}{U_0^4 \rho_a \rho_L}\right)^{\frac{1}{6}} \left[1 + 2.6 \mu_L \cos \theta \left(\frac{h_0^2 \rho_a^4 U_0^7}{72 \rho_L^2 \sigma^5}\right)^{\frac{1}{3}}\right]^{0.2} \quad (16)$$

Velocity of the liquid at the atomizer tip (U_0) is given by

$$U_0 = \sqrt{\frac{2\Delta P_L}{\rho_L}} \quad (17)$$

Since the Sauter Mean Diameter (SMD) of the spray depends on surface area, the evaporation effects of the spray also to be considered and is given by

$$SMD = 2.25 \sigma^{0.25} \mu_L^{0.25} \dot{m}_L^{0.25} \rho_a^{-0.25} \Delta P_L^{-0.25} \quad (18)$$

III. RESULTS AND DISCUSSIONS

From the above theoretical relations, the spray characteristics and the flow parameters are calculated by fixing a mass flow rate of 0.006 kg/s and a pressure differential of 4 bar. The diameter of the nozzle exit orifice (D_0) is selected as 2mm. Liquid water at room temperature is selected as the fluid flowing through the atomizer and air is selected as the continuous medium which is filled in the atomizer. The flow parameters and spray characteristics are calculated and the results are tabulated below.

TABLE I. THEORETICAL RESULTS OF SPRAY MODELLING

Flow Variable/Spray Characteristic	Value
Flow Number, FN	$3 \times 10^{-7} \text{m}^2$
Liquid sheet thickness, h_0	$4.534 \times 10^{-5} \text{m}$
Velocity at the tip, U_0	28.284 m/s
Ligament diameter, D_L	15.03 μm
Discharge Coefficient, C_d	0.675
Spray semi angle, θ	32.64°
Sauter Mean Diameter, SMD	35.406 μm .

The computational results of the spray modelling is determined by using some of the parameters obtained above and the other spray characteristics are found numerically for different conditions of injection. The pressure differential applied on the injector is varied from 2 bar to 6 bar. The mass flow rate of liquid flowing through the atomizer is found to be increasing as the injection pressure differential increases. As the mass flow rate and injection pressure differential increases, the spray semi angle increases and hence the atomization quality goes on increasing. The variation of spray semi angle with the injection pressure differential is shown in figure-4.

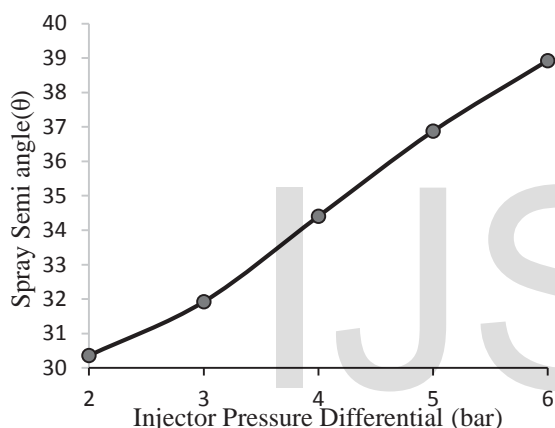


Fig. 4. Spray semi angle as a function of injection pressure differential

The Sauter Mean Diameter (SMD) of the spray, which is the diameter of a drop having the same surface to volume ratio as the mean value for the entire spray, is found to be decreasing, which is an implication of the increase in atomization quality. The increase in the liquid pressure differential causes the liquid to be discharged from the nozzle at a high velocity, which promotes a finer spray. At high flow velocities, the droplet diameter becomes smaller due to better atomization. In practice, the significance of the surface tension is negligible. Most commercial fuels exhibit only a slight difference in this property. The swirling motion of the flow in the swirl chamber helps in creating the air core at the centre spray axis due to the centrifugal motion of the liquid in the swirl chamber, and by confining the liquid at the walls of the swirl chamber. The path lines at the inlet and wall of the pressure swirl nozzle clearly depicts the swirling motion of the liquid and the creation of the central air core at the central axis of the atomizer. The path lines at the inlet of the atomizer is shown in figure 5 below.

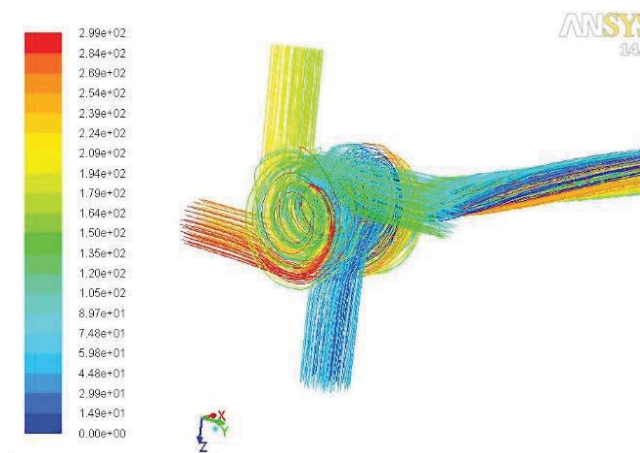


Fig.5. Path lines at the inlet showing swirling motion and formation of air core

The particle tracks obtained from the numerical solution of the coupled flow in terms of the particle diameter of the droplets in the spray domain is shown in figure-6 below.

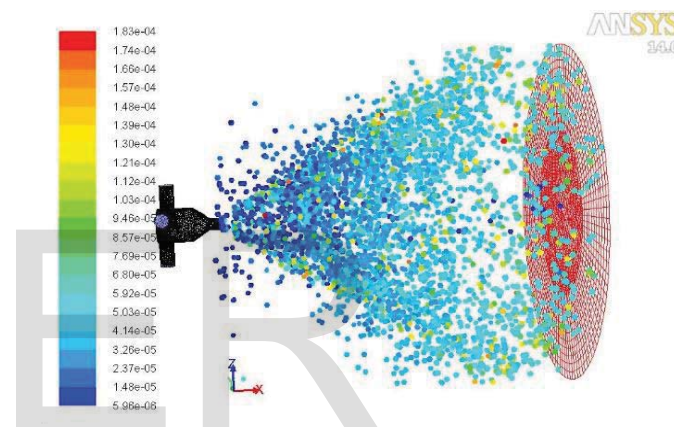


Fig. 6. Particle tracks colored by particle diameter

From the particle tracks of pressure swirl atomizers, it is observed that the spray particles are distributed with in a spray semi angle of 33°. Also the particle diameter of most of the spray particles are in the range of 10 μm to 90 μm (0.01 mm to 0.09mm), which is typically in the range of particle diameters of pressure swirl atomizers. The injection summary for the pressure swirl atomizers, which gives the other spray characteristics is given below.

TABLE II. INJECTION SUMMARY FROM THE ATOMIZER

Injection Characteristics	Value
Total number of parcels	11603
Total number of particles	1.624e+06 (m)
Maximum particle diameter	1.834e-04 (m)
Minimum particle diameter	5.514e-06 (m)
Overall mean diameter	2.132e-05 (m)
Overall Sauter diameter	4.21e-05 (m)

The overall sauter mean diameter (SMD) obtained numerically is in close agreement with the theoretical estimates. The variation of particle diameter in the external spray domain is in the range of 15µm to 60µm, which implies that the atomization quality has increased considerably in the spray domain for the given flow conditions of the atomizer, especially in the region close to the nozzle exit orifice. The variation of droplet diameter (droplet diameter distribution) in the external spray domain is shown below.

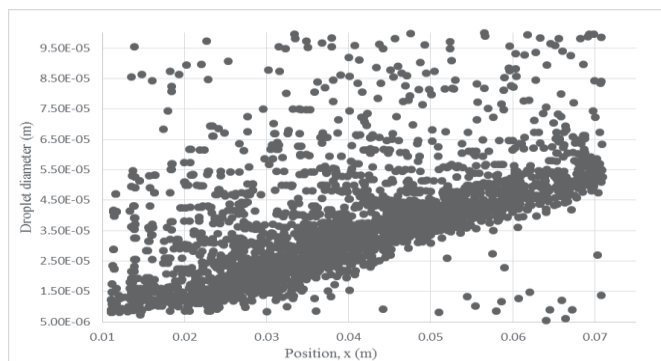


Fig.7. Droplet diameter distribution in the external spray domain

The injection pressure differential was varied from 2 bar to 8 bar and the SMD values have been found out and it was observed that the SMD of the spray has decreased considerably with the increase in injection pressure. If SMD has a low value, the evaporation will increase. SMD does not present any information about the distribution of the droplet size. In other words, two sprays with the same SMD may have different droplet distribution. The plot showing the variation of SMD with increase in injection pressure is in figure-8 below.

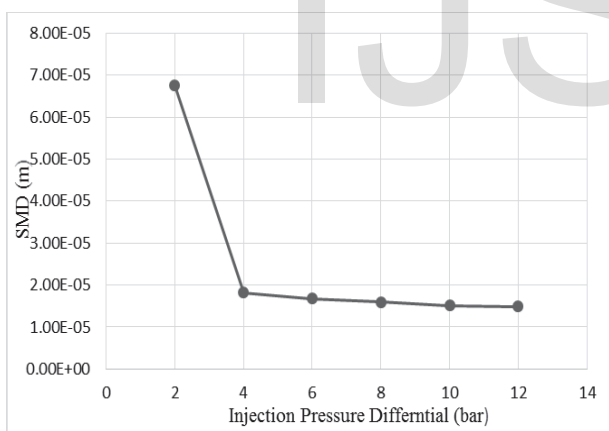


Fig.8. Variation of SMD with injection pressure

IV. CONCLUSIONS

The spray modelling from pressure swirl atomizer is done with CFD code Fluent using the Lagrangian approach by setting atomizer characteristics like Sauter Mean Diameter (SMD), spray cone angle, exit velocity, drop size distributions etc. are determined numerically and compared with the theoretical estimates and most of the results are in agreement except a slight difference in SMD. The discrepancy may be due to the

difference in assumptions in developing the relations for various spray characteristics. The results obtained from the theoretical formulation and the numerical modelling is tabulated below.

TABLE III. COMPARISON OF RESULTS

	SMD	Exit Velocity	Spray semi angle
Theoretical	35.41µm	28.284 m/s	32.64°
Numerical	42.10 µm	30.58 m/s	34.86°

In this work only one atomizer was investigated and this was done in a limited range of injector pressure differentials, the comparison of parameters at the point ($\Delta P = 4$ bar and $m_L = 0.006$ kg/s) is done. For more conclusive results it would be interesting to compare different injection conditions.

References

- [1] M.R. Halder, S.K. Dash And S.K. Som, "Initiation of air core in a simplex nozzle and the effects of operating and geometrical parameters on its shape and size," *Experimental Thermal and Fluid Science*, pp.871-878, 2002
- [2] Lefebvre A H., "Atomization and Sprays." Hemisphere Publishing Corporation, New York, 1989
- [3] Pedro Teixeira Lacava., Demétrio Bastos-Netto., and Amílcar Porto Pimenta. "Design and experimental evaluation of pressure-swirl atomizers," *24th International Congress of the Aeronautical Sciences*, Instituto Tecnológico de Aeronáutica, Brazil, 2004.
- [4] A. Datta., and S.K. Som., "Numerical prediction of air core diameter, coefficient of discharge and spray cone angle of a swirl spray pressure nozzle," *International Journal of Heat and Fluid Flow*, pp. 412-419, 2000
- [5] Ahmad Hussein., Abdul Hamid., and Rahim Atan, Spray characteristics of jet-swirl nozzles for thrust chamber injector, *Aerospace Science and Technology*, pp. 192-197. 2008
- [6] Jesper Madsen., "Computational and Experimental Study of Sprays from the Breakup of Water Sheets," Thesis, Aalborg University, Denmark, 2006.
- [7] Halder M.R, and Som S.K., "Numerical and Experimental Study on Cylindrical Swirl Atomizers," *Atomization and Sprays*, Vol.16, pp. 223-236, 2006
- [8] Vivek Kumar., Shitalkumar Joshi., Jochen Schuetze., Markus Braun and Muhammad Sami, "Modeling Primary Atomization," *ILASS Americas, 25th Annual Conference on Liquid Atomization and Spray Systems*, Pittsburg, USA, 2013
- [9] John.J.Chinn, Andre.J.Yul, "Computational Analysis of swirl atomizer internal flow", University of Manchester Institute of Science and Technology (UMIST), Manchester, England, 2012
- [10] A. BelhadeF., A. Vallet., M. Amielh., and F. Anselmet, "Pressure Swirl Atomization: Modelling and Experimental Approaches," *International journal of Multiphase Flow*, pp. 13-20, 2012